



Published in final edited form as:

Cell Stem Cell. 2012 April 6; 10(4): 455–464. doi:10.1016/j.stem.2012.01.021.

Human Embryonic Stem Cell-Derived GABA Neurons Correct Locomotion Deficits in Quinolinic Acid-Lesioned Mice

Lixiang Ma, Baoyang Hu, Yan Liu, Scott Christopher Vermilyea, Huisheng Liu, Lu Gao, Yan Sun, Xiaoqing Zhang, and Su-Chun Zhang

Abstract

Degeneration of medium spiny GABA neurons in the basal ganglia underlies motor dysfunction in Huntington's disease (HD) which presently lacks effective therapy. In this study, we have successfully directed human embryonic stem cells (hESCs) to enriched populations of DARPP32-expressing forebrain GABA neurons. Transplantation of these human forebrain GABA neurons and their progenitors, but not spinal GABA cells, into the striatum of quinolinic acid-lesioned mice results in generation of large populations of DARPP32⁺ GABA neurons, which project to the substantia nigra as well as receiving glutamatergic and dopaminergic inputs, corresponding to correction of motor deficits. This finding raises hopes for cell therapy for HD.

INTRODUCTION

Huntington's disease (HD) is an inherited degenerative disorder with cognitive and psychiatric impairments as well as chorea movements. The motor dysfunction is primarily associated with degeneration of γ -aminobutyric acid (GABA) medium spiny neurons (MSN) in the basal ganglia due to abnormal expansion of cytosine-adenine-guanine (CAG) repeats within the genome leading to a malfunctioning huntingtin protein. Significant efforts have been placed in reducing the numbers of CAG repeats through genetic inhibition of the pathologic CAG repeats, though balancing the removal of pathologic and maintenance of normal CAG is likely not trivial (Johnson and Davidson, 2010). Presently, no disease-modifying therapy is on the horizon for this debilitating disorder.

An alternative strategy is to replace the degenerated GABA neurons in the basal ganglia (Dunnett and Rosser, 2007). Unlike in Parkinson's disease in which tonic supplementation of dopamine by dopamine-producing cells may provide beneficial effects, in HD reformation of circuitry is necessary (Campbell et al., 1993; Goto et al., 1997; Mazzocchi-Jones et al., 2011; Nakao and Itakura, 2000). Transplanted GABA neurons must project to and receive from their target tissues, consisting of the globus pallidus and substantia nigra, as well as inputs from the cerebral cortex (Wictorin, 1992) in order to achieve functional benefits. This is a relatively long distance for grafted neuronal axons to travel in the adult brain environment, which becomes a major obstacle of cell therapy (Bonner et al., 2010; Pfeifer et al., 2004). Nevertheless, fetal striatal tissue transplantation into the quinolinic acid (QA)-lesioned rodent or nonhuman primate brain has yielded improvements in motor deficits (Dobrossy and Dunnett, 2006; Palfi et al., 1998; Pearlman et al., 1993; Wictorin et al., 1990). Such results prompted clinical trials using fetal tissue transplantation (Bachoud-

Publisher's Disclaimer: This is a PDF file of an unedited manuscript that has been accepted for publication. As a service to our customers we are providing this early version of the manuscript. The manuscript will undergo copyediting, typesetting, and review of the resulting proof before it is published in its final citable form. Please note that during the production process errors may be discovered which could affect the content, and all legal disclaimers that apply to the journal pertain.

The authors state that they have no competing financial interests.

Levi et al., 2000; Hauser et al., 2002; Philpott et al., 1997; Rosser et al., 2002) with clinical benefits in some patients receiving bilateral striatal allografts (Bachoud-Levi et al., 2006; Gallina et al., 2010; Reuter et al., 2008). However, clinical application of transplant therapy is plagued by lack of a consistent source of human MSN, which presents yet another roadblock for therapeutic application.

Human pluripotent stem cells (hPSCs), including human embryonic (hESCs) and human induced pluripotent stem cells (hiPSCs) (Takahashi et al., 2007; Thomson et al., 1998), are potential sources of MSNs. Differentiation of GABA neurons from hESCs or hiPSCs was explored but the differentiation efficiency of striatal GABA neurons was low (Aubry et al., 2008; Zhang et al., 2010) and transplantation of these cells into QA-lesioned rats lead to tumor formation or overgrowth (Aubry et al., 2008), suggesting a critical need of efficiently restricting stem cells to the MSN fate. In the present study, we have successfully directed hESCs to enriched populations of GABA MSNs. Importantly, these human GABA neurons, following transplantation into the striatum of QA-lesioned mice, project to the substantia nigra as well as receiving glutamatergic and dopaminergic inputs, corresponding to correction of motor dysfunction.

RESULTS

LGE-like progenitors are efficiently induced from hESCs by SHH

Medium spiny GABA neurons originate from lateral ganglionic eminence (LGE) (Campbell, 2003; Olsson et al., 1995; Wichterle et al., 2001; Wilson and Rubenstein, 2000). LGE progenitors express *Gsx2*, *Ctip2*, and *Meis2*, and, to a lesser degree, *Pax6* but not *Nkx2.1* (Arlotta et al., 2008; Fode et al., 2000; Puelles et al., 2000; Toresson et al., 2000). We hypothesized that LGE progenitors are specified from hESCs under a specific level of SHH. hESCs were differentiated for 10-12 days to generate primitive neuroepithelial cells (Pankratz et al., 2007), which were then exposed to SHH (0, 100, 200, 500, and 1,000 ng/ml) from day 12 to 26 (Figure 1A). Immunostaining indicated that SHH reduced both the level and proportion of *Pax6*, while increased those of *Nkx2.1* and *Meis2* in a dose-dependent manner (Figures 1B, 1C, 1D **and not shown**), but did not affect the levels of *Otx2* and *FoxG1*, transcription factors of the anterior neuroectoderm (Figures 1G, **and not shown**). At 200 ng/ml, SHH optimally reduced the *Pax6*-expressing cells to $40.1 \pm 1.9\%$ and increased *Mash1* positive cells to $56.4 \pm 1.3\%$, yet minimally elevated the *Nkx2.1* population ($30.2 \pm 0.9\%$) (Figures 1B, 1C, 1F and 1G). These results suggest that the majority of progenitors are characteristic of LGE cells with the application of 200 ng/ml of SHH. It should be noted that *Pax6* is also expressed in the LGE although the level of expression is lower than that in the cortex (Flames et al., 2007; Yun et al., 2001). Therefore, the low-*Pax6*-expressing cells under 200 ng/ml SHH (Figure 1B) are likely LGE-like progenitors. Indeed, *Meis2*, a transcription factor that is enriched in striatal GABA progenitors (Toresson et al., 2000), was highly induced ($89.7 \pm 2.3\%$) by SHH at this dosage (Figures 1D, 1F and 1G). mRNA expression of *Gsx2*, a transcription factor expressed primarily in the LGE (Toresson and Campbell, 2001; Yun et al., 2001), increased drastically (Figure 1E). Thus, with a medium dosage of SHH, hESCs can be efficiently directed to ventral neural progenitors which bear characteristics of early LGE cells, thereafter referred to as LGE-like progenitors.

We have previously shown that a small molecule, purmorphamine, can replace SHH in differentiating hESCs to ventral neural progenitors (Hu et al., 2009; Li et al., 2008). Dose-dependent assays revealed purmorphamine at $0.65 \mu\text{M}$ to be equivalent to SHH at 200 ng/ml for generating LGE-like progenitors (Figures 1F and 1G). We therefore used purmorphamine ($0.65 \mu\text{M}$) and SHH (200 ng/ml) interchangeably for patterning neuroepithelia to LGE-like progenitors.

LGE-like progenitors generate predominantly DARPP32-expressing GABA neurons

The LGE-like progenitors in suspension were exposed to VPA from day 26 for 6 days without SHH or purlmorphamine before they were dissociated for neuronal differentiation on laminin substrate at day 32 (Figure 2A). Two weeks after plating (day 47), the majority of cells ($93.2 \pm 3.5\%$) were process-bearing neurons, as revealed by phase contrast imaging and by positive immunostaining for β III-tubulin. Among β III-tubulin+ neurons, $90.2 \pm 4.2\%$ were positive for GABA (Figures 2B and 2C), whereas very few cells ($1.2 \pm 0.8\%$) were positive for choline acetyltransferase (ChAT), which are derived from MGE progenitors. Importantly, the majority of the GABA neurons ($89.7 \pm 8.3\%$) were positive for dopamine- and cAMP-regulated phosphoprotein of 32 kDa (DARPP32) (Figures 2B and 2D), a feature of MSNs (Ouimet et al., 1984). If the MGE-like progenitors, generated in the presence of 500 ng/ml SHH, were differentiated, few of the neurons were positive for DARPP32 (Figures 2B and 2D). In contrast, if the ventral progenitors were caudalized by retinoic acid (RA) between day 10 and 23, a similar population of GABA neurons ($81.2 \pm 7.1\%$) were generated but they were negative for DARPP32 (Figures 2B, 2C and 2D). Therefore, a specific concentration of SHH is required to specify LGE-like progenitors which subsequently generate DARPP32+ GABA neurons. These GABA neurons possessed numerous spines on their dendrites and were also positive for Meis2, and GAD65/67 (Figures 2E and 2F), an enzyme required for GABA synthesis. These results suggest that the GABA neurons generated in the presence of 200 ng/ml SHH or 0.65 μ M purlmorphamine possess the phenotypes of typical striatal MSNs.

HPLC measurement of media conditioned by 90-day-old cultures indicated that the cultured neurons released measurable amount of GABA, whereas neurons differentiated without SHH, which are primarily glutamatergic neurons and some GABA interneurons (Li et al., 2009), or those differentiated in the presence of RA, which represent ventral spinal neurons including motor neurons and GABA interneurons, produced much lower concentrations of GABA. Stimulation of the cultures with a high-potassium solution, which depolarizes neurons, resulted in over 6-fold increase in GABA release (Figure 2G), confirming the GABAergic identity and the capacity of these neurons to release GABA in response to stimuli. Given the similar numbers of GABA neurons in striatal and spinal cultures, this result indicates that stem cell-derived striatal GABA neurons possess a higher capacity in releasing GABA than GABA interneurons.

Whole cell patch clamping recording of 70-day-old cultures revealed action potentials elicited by injection of current steps from +20 nA to +80 nA besides membrane properties characteristic of an active neuron (Figures 2H and Figure S1). Interestingly, spontaneous synaptic activity was nearly completely blocked by bicuculline alone (Figure 2H), reflecting primarily inhibitory (GABA) neurotransmission inputs in our cultures. This was corroborated by the fact that 16 out of 18 (biocytin-labeled) recorded cells were positive for GABA (Figure S1C).

The hESC-derived progenitors survive and produce GABA neurons in the lesioned striatum

To determine if the *in vitro* produced human GABA neurons exhibit functional properties of GABA MSNs and if they possess therapeutic potential for HD, we transplanted the LGE-like progenitors (maintained in suspension culture for 40 days), into the striatum of immune deficient SCID mice lesioned by QA, a model commonly used for testing efficacy of donor cells (Sanberg et al., 1989). Spinal GABA neural progenitors, which generated a similar proportion of GABA neurons *in vitro*, were used as a control. The QA-lesioned striatum exhibited a significant loss of neurons, as revealed by NeuN staining (Figure S2B), and near complete lack of DARPP32-expressing GABA projection neurons at 4 weeks post QA

injection, giving the appearance of a shrunk striatum and enlarged ventricle on the lesion side (Figure S2A).

Four months after transplantation, both the forebrain and the spinal GABAergic cells repopulated the shrunk striatum, giving a symmetrical image of the brain viewed from cross sections. DNA dye staining showed no obvious disruption of the striatal structure. Immunostaining for human nuclei (hN) indicated that the human cells are primarily distributed in the lesion striatum (Figure 3A). Stereological measurement showed an average of $3,466,667 \pm 648,931$ ($n=10$) in the forebrain neuron (FBN) group and $3,179,245 \pm 452,133$ ($n=10$) in the spinal neuron (SPN) group (Figure 3E). Hence there was no obvious difference in graft size between the forebrain and spinal cell transplants.

Examination of neuronal phenotypes revealed a large populations of GABA-expressing neurons in both the forebrain ($62.8 \pm 2.6\%$) and spinal ($66.8 \pm 3.4\%$) grafts (Figure 3B). There was no obvious difference in the numbers of GABA-expressing neurons between the groups (Figure 3E). Nevertheless, most of the cells in the forebrain, but not spinal, cell grafts were positive for striatal GABA projection neuronal markers, Meis2, DARPP32 (Figures 3B and 3C), and Ctip2 (**not shown**). The fluorescent intensity of DARPP32 was variable and much lower than that of endogenous striatal GABA neurons but these cells were present throughout the grafted striatum (Figure 3C). The GABA neurons in the forebrain cell grafts were larger and multipolar whereas those in the spinal cell grafts were smaller and less branched (Figures 3D and 3F). The former also possesses numerous dendritic buttons along the MAP2+ dendrites, as revealed by human specific synaptophysin staining (Figure 3D). Stereological measurement estimated that DARPP32-expressing GABA neurons constitute $58.6 \pm 3.0\%$ of total grafted cells in the FBN group, in comparison to none in the SPN group (Figure 3E). Like endogenous striatal GABA neurons (Durieux et al., 2011), the grafted human striatal GABA neurons also expressed enkephalin or substance P (Figure S3). Therefore, while both forebrain and spinal progenitors generate similar numbers of GABAergic neurons, only the forebrain progenitors differentiate to GABA neurons with the striatal projection phenotypes.

While the vast majority of the grafted cells become β III-tubulin+ neurons ($86 \pm 4.04\%$), some ($8.43 \pm 1.42\%$) became astrocytes (Figures S4A and S4B). Besides GABA neurons being the predominant population, small populations of neurons were present in the forebrain neuron (FBN) grafts that expressed ChAT ($1.57 \pm 0.41\%$), vGLUT1 ($0.92 \pm 0.15\%$), 5-HT ($0.86 \pm 0.27\%$), and TH ($0.97 \pm 0.29\%$) (Figures S4C and S4D). Although the majority of neurons were DARPP32-expressing projection neurons, $6.0 \pm 0.52\%$ of total cells were positive for calbindin (Figures S4E and S4F), a calcium binding protein (Kawaguchi et al., 1995). Interestingly, two-thirds of them, or $3.89 \pm 0.57\%$ of the total cells, did not colabel with GABA (Figures S4G and S4H). In addition, $1.05 \pm 0.22\%$ for calretinin, $1.02 \pm 0.16\%$ were positive for parvalbumin, and $0.50 \pm 0.07\%$ for somatostatin and they were all positive for GABA (Figures S4E and S4F). Immunostaining for neural progenitor marker nestin and mitotic marker KI67 showed a lack of mitotic progenitors in the grafts 4 months after transplantation although at one week after transplantation, KI67 positive cells were present (Figure S4I). At one week, the majority of the cells were nestin-positive but Pax6-negative progenitors with few ($2.4 \pm 0.72\%$) DARPP32 positive GABA neurons (Figure S4J), suggesting that the majority of the GABA neurons are generated from grafted progenitors.

Human GABA neurons connect with endogenous cells

Striatal GABA projection neurons reciprocally synapse with neurons in the globus pallidus, thalamus, and substantia nigra, thus regulating locomotion (Victorin, 1992). Confocal analyses showed that grafted GABA neurons in both groups colabeled with PSD95 (Figure 4A), suggesting that the grafted GABA neurons receive potential inputs. Further labeling

showed robust TH staining on GABA⁺ cell bodies and processes in the forebrain cell graft but not in the spinal cell transplant (Figure 4A), suggestive of dopaminergic inputs into the grafted MSN, possibly from the midbrain. Double staining also revealed dense vGlu signals on forebrain GABA neurons but substantially less in spinal GABA neurons (Figure 4A), suggesting glutamatergic inputs, possibly from cortex, globus pallidus, and/or thalamus. Since GABA neurons are almost completely destroyed in the lesion site and since there are few TH⁺ dopamine neurons and vGlu⁺ glutamate neurons in the graft (Figures S4C and S4D), colabeling of TH or vGlu on GABA neurons suggests inputs from endogenous neurons. This is confirmed by lack of labeling of (human specific) STEM121 on TH- or vGlu-expressing fibers (**lower row in Figure 4A**).

In the anterior substantia nigra, a discrete bundle of (human specific) synaptophysin-expressing fibers were observed in the FBN group but not the SPN group. These fibers overlapped with TH-expressing neurons (Figure 4B), indicating that the grafted human GABA neurons project to the anterior substantia nigra and potentially form connections with dopaminergic neurons. In this area, the DARPP32 fibers also expressed substance P but none of them expressed enkephalin (Figure 4B), suggesting specific projection by subtype-specific DARPP32-expressing GABA neurons. These results confirm the projection nature of the grafted human forebrain GABA neurons and their ability to project to appropriate targets.

Transplantation of forebrain but not spinal GABA progenitors corrects motor deficits

Besides rotarod and open field tests, we employed an unbiased motor tests using Treadscan which not only reveals limb movements detected by skilled paw use tests but also shows characteristic chorea movement behaviors that are features of Huntington patients (Menalled et al., 2009). Unilateral QA-induced striatal lesion resulted in motor deficits typical of HD, including decreased latency in rotarod test, decreased center ratio/crossings in open field test, and changes in a number of parameters of fine gait movements revealed by Treadscan such as smaller stride length (the distance between two successive initiations of stances) but a larger foot base (distances between front and rear foot pair), increased minimum lateral deviation (the closest distance from foot to the body axis), and increased maximum longitudinal deviation (the farthest distance of foot away from the body axis, equivalent to the ataxic gait of a HD patient). The small stride length, lagging and wobbling of rear limbs resemble the gait abnormalities seen in typical HD patients (Koller and Trimble, 1985; Vandeputte et al., 2010).

Monthly Behavioral analysis post transplantation (Figure 5A) revealed that mice receiving the forebrain but not spinal GABA progenitor transplantation exhibited increased latency on rotarod (Figure 5B) and increased center ratio, crossings and total distance in open field tests (Figure 5C). Gait analysis with Treadscan indicated that mice receiving forebrain GABA progenitors exhibited a significantly greater stride length. The maximum longitudinal deviation, minimum lateral deviation and the foot base of their rear limbs, especially on the right (lesion) side, became smaller over time (Figure 5D). These results indicate that the forebrain, but not spinal, GABA neurons correct the locomotion deficits in the QA-lesioned mice.

DISCUSSION

By following the developmental principles and by tuning a particular dose of SHH or purmorphamine on primitive neuroepithelia, we have directed hESCs to an enriched population of LGE-like progenitors, which differentiate to predominantly DARPP32-expressing MSNs *in vitro* and *in vivo*. Importantly, the human stem cell-derived MSNs, but not the DARPP32 negative GABA interneurons, project to the substantia nigra and possibly

also receive from neurons in the cerebral cortex and substantia nigra, which corresponds to correction of locomotion deficits in the QA-lesioned mice. These results raise the prospect of cell based therapy as a potential treatment for HD, given the complete lack of effective treatment for HD at the present.

Differentiation of MSNs from hESCs was explored by Perrier and colleagues (Aubry et al., 2008). They generated approximately 8% GABA⁺ and 12% DARPP32⁺ neurons among the differentiated progenies in the presence of both SHH and a Wnt inhibitor DKK1. Transplantation of these cells, either at day 45 or 56, invariably leads to overgrowth 13-15 weeks post-graft (Aubry et al., 2008). A number of factors may explain the contrasting outcomes between our results, ranging from culture modes to use of morphogens (timing, concentration, combinations, etc). As we have demonstrated in the present study, a specific concentration of SHH is necessary to induce neuroepithelia at a particular window of development in order to induce a synchronized population of LGE-like progenitors, which give rise to DARPP32-expressing MSNs. Less or over ventralization of primitive NSCs will lead to generation of cortical or MGE neuronal types, respectively (Danjo et al., 2011; Li et al., 2009), demonstrating the precise regulation of cell fate specification by extracellular signals. Exposure of monolayer neuroepithelial colonies to morphogens under our chemically defined culture, instead of neurospheres derived from co-culture with PA6 stromal cells (Aubry et al., 2008), may further account for the synchronized population of LGE-like progenitors and MSNs. It may seem surprising to produce a large population of DARPP32 MSNs given the presence of a substantial proportion of Pax6- and Nkx2.1-expressing progenitors. It should be noted that Pax6 is also expressed in the LGE although the expression level is lower than that in the cortex (Flames et al., 2007; Yun et al., 2001). Indeed, under 200 ng/ml SHH the Pax6 fluorescent intensity is much lower (Figure 1B); hence they are likely LGE-like progenitors. This is supported by a complete lack of Pax6-expressing cells at one week post transplantation and few glutamatergic neurons in the grafts 4 months post-graft. The Nkx2.1 progenitors can produce cholinergic neurons and GABA interneurons (Sussel et al., 1999), but our differentiation culture (without NGF) does not favor generation/survival of cholinergic neurons. It is also suggested by the observation that only about 5% of the total grafted cells express GABA and other interneuronal phenotypes, parvalbumin, calretinin, and somatostatin. Together, this progenitor pool produces the most robust population of DARPP32-expressing GABA neurons in vitro and in vivo, as evidenced by electrophysiological and transplant results. Our method was also effective in differentiating MSNs from iPSCs (**not shown**), thus facilitating studies of MSN degenerative processes, especially with those from HD iPSCs (Zhang et al., 2010).

HD remains a devastating condition due to a near complete lack of effective therapy. Clinical trials with fetal cell transplantation suggest that cell therapy is a potential promising option for HD if a consistent donor source is available (Clelland et al., 2008; Gallina et al., 2010). While the QA-lesioned mice do not completely mimic the pathology of HD, they offer a simple model to examine the efficacy of cell therapy. It is encouraging that grafted human neural progenitors repopulated the atrophied striatum, differentiated to GABAergic neurons, and contributed to correction in movement impairments. Our parallel comparison of two different populations of human GABA progenitors provides insights into the biology and potential use of GABA neurons in HD treatment. First, GABA MSNs are required for correcting the motor deficits. A simple provision of GABA or GABA-producing cells, such as the GABA interneurons in the present study, is not effective for correcting the motor deficits. Second, therapeutic outcome may be dependent upon the reformation of circuitry by grafted GABA neurons. While the GABA interneurons can form connections with each other and potentially also with host neurons, they do not project out of the striatum. In contrast, the human GABA MSNs not only receive inputs but also project outside of the graft site. More importantly, these GABA neurons appear to receive specific inputs,

including dopaminergic and glutamatergic inputs, and project to specific brain regions-- substantia nigra. And the projection appears specific to the substance P- but not enkephalin-expressing GABA neuronal subtype, resembling the endogenous striatal GABA neurons (Gerfen, 1988). These phenomena strongly suggest the intrinsic capacity of appropriately patterned developing neurons to find their target and the reformation of neural circuitry, which may underlie the correction of motor deficits. Third, the adult CNS environment is generally inhibitory to axonal regeneration. However, our present observations indicate that the human stem cell-derived neurons can project for quite a distance. Indeed, human fetal striatal cells transplanted into a similar QA-lesioned rat striatum could project to the substantia nigra (Victorin et al., 1990). The striking similarity between fetal human striatal cells and our in vitro produced striatal cells validates the identity and utility of our stem cell-produced GABA neurons. It would be interesting to replicate these cellular behaviors in other models such as the newly established transgenic HD model that has clear striatal GABA neuron degeneration (Wilburn et al., 2011).

One of the main obstacles to stem cell therapy is tumor formation or overgrowth (Aubry et al., 2008; Roy et al., 2006). The grafts from both the forebrain and the spinal GABA neuronal progenitors do not appear disruptive to the striatal structures nor do they remain proliferating progenitors. Multiple factors may contribute to such an outcome. Our initial adherent colony neural induction culture mode allows obtaining a nearly pure population of neuroepithelia (Hu et al., 2010; Zhang et al., 2001), and subsequent patterning with SHH effectively restricts the cells to a ventral progenitor fate. Expansion of the progenitors for additional two weeks also significantly decreases cell cycle numbers needed for the grafted human progenitors to produce neurons. This is evidenced by the fact that at least 94% of the grafted cells are neurons and astrocytes and the majority of the neurons are of GABA phenotypes. It is no doubt that rigorous testing in more animals for a longer period is necessary to move to clinic trials, however, the present finding, particularly the ability of hESC-derived GABA MSNs to receive and project to specific targets, raises hopes for cell based therapy for HD.

EXPERIMENTAL PROCEDURES

Differentiation of forebrain and spinal GABA neurons from hESCs

hESCs (line H9, passages 21- 42; line H1, passages 24-34) were maintained on a feeder layer of irradiated mouse embryonic fibroblasts (MEFs) as described (Thomson et al., 1998). hESCs were differentiated to Pax6-expressing primitive neuroepithelia (NE) for 10-12 days in a neural induction medium consisting of DMEM/F12, N2 supplement and non-essential amino acids (Pankratz et al., 2007; Zhang et al., 2001). Sonic hedgehog (SHH, 50-500 ng/ml) or its small molecular agonist purmorphamine (0.1-1.5 μ M, Calbiochem, San Diego, CA, USA) was added at days 12-26 to induce ventral progenitors. For generating spinal GABA neurons, retinoic acid (RA, 0.1 μ M) was added from day 10 -23 (Li et al., 2008). For neuronal differentiation, neural progenitor clusters were dissociated with Accutase (1 unit/ml, Invitrogen) at 37°C for 5 minutes and placed onto poly-ornithine/laminin-coated coverslips at day 26 in Neurobasal medium in the presence of valproic acid (VPA, 10 M, Sigma) for 1 week, followed by a set of trophic factors, including brain derived neurotrophic factor (BDNF, 20 ng/ml), glial-derived neurotrophic factor (GDNF, 10 ng/ml), insulin-like growth factor 1 (IGF1, 10 ng/ml), and cAMP (1 μ M) (all from R&D Systems). Detailed differentiation procedure is presented in supplementary information.

Immunocytochemistry and quantification

Coverslip cultures were fixed in 4% paraformaldehyde for 15 min at 4°C, washed with PBS and incubated in a blocking buffer (10% donkey serum and 0.2% triton X-100 in PBS) for

60 minutes at room temperature before being incubated in the following primary antibodies (Table S1) overnight at 4°C. Fluorescently conjugated secondary antibodies were used to reveal the binding of primary antibodies (1:1000, Jackson, West Grove, PA) and nuclei were stained with Hoechst 33258. Images were collected using a Nikon TE600 fluorescence microscope (Nikon Instruments, Melville, NY, USA) or a Nikon C1 laser-scanning confocal microscope (Nikon, Tokyo, Japan). The population of Otx2, Pax6, Nkx2.1 and Mash1 expressing cells among total differentiated cells (Hoechst-labeled) was counted using ImageJ software. At least five fields of each coverslip were chosen randomly and three coverslips in each group were counted. Data were replicated three times in two different cell lines (H9 and H1) and were expressed as mean±s.e.m..

RNA isolation and quantitative PCR

The total RNA was isolated from cultured cells using RNA STAT-60 (Tel-Test, Friendswood, TX, USA). cDNA was generated from 1 g of total RNA using the SuperScript III First-Strand Synthesis System (Invitrogen, Carlsbad, CA, USA) and was used as a template for the quantitative PCR (qPCR).

Measurement of GABA release by HPLC

Cultured cells were washed four times with Krebs'–Ringer's solution containing 130 mM NaCl, 3mM KCl, 2mM CaCl₂, 0.8mM MgSO₄, 10mM glucose, and 20 mM HEPES (pH 7.4) before the medium was collected with depolarizing Krebs'–Ringer's solution contained 83 mM NaCl, 50 mM KCl, 2mM CaCl₂, 0.8mM MgSO₄, 10mM glucose, and 20 mM HEPES (pH 7.4). The collected media were then mixed with o-phthalaldehyde (0.8g/L) and 2-mercaptoethanol (2 ml/L) for 5 min at 15 C. Samples were then injected into the HPLC system and analyzed using a fluorescence monitor (excitation at 350 nm, emission at 450 nm) (CMA/Microdialysis, Stockholm, Sweden). The mobile (60 µl /min) solution consisted of (in mM) 100 KH₂PO₄, 100 Na₂HPO₄, and 0.1 EDTA, pH6.0, contained 10% acetonitrile and 3% tetrahydrofuran. The peak area at the predicted position was calibrated against the standard curves for quantification with CMA200 software (CMA/Microdialysis).

Whole cell patch clamp recording

Whole-cell patch-clamp recordings were performed on hESC-derived neurons that were differentiated for 8-10 weeks as described (Johnson et al., 2007). The identity of recorded cells was revealed by injecting biocytin (1%, Sigma) followed by immunostaining.

Striatal Lesions and Cell Transplantation

All animal experiments were conducted according to a protocol approved by the animal care and use committee at University of Wisconsin-Madison. To create the unilateral lesion, adult male SCID mice (10 weeks of age) were anesthetized with 1–2% isoflurane mixed in oxygen, and received a stereotaxic injection of 2µl of 0.1M quinolinic acid (QA, P63204; Sigma, in saline with 0.2mg/ml ascorbic acid) into the right striatum on a coordinator (anterior-posterior (AP) =−0.7 mm, lateral (L)=+1.7 mm, vertical (V) =−3.2mm) (Hansson et al., 1999).

Differentiated forebrain or spinal GABA neuron progenitors (40 days of differentiation from hESCs in suspension) were dissociated with Accutase and prepared at approximately 50,000 cells/µl in artificial cerebrospinal fluid (aCSF) containing B27, 200 mM ascorbic acid, 1 mM cAMP, 20 ng/ml BDNF, and 10 ng/ml GDNF. Cell suspension (2 µl) was injected into the lesioned striatum (AP =−0.8 mm, L=+2.0 mm, V =−3.2mm) of anesthetized animals 4 weeks after QA lesion using a glass pipette (0.3–0.5 mm in diameter) over a period of 5

minutes. The QA-lesioned animals receiving the same surgery and injection of 2 μ l of the same aCSF solution (without cells) served as controls.

Behavioral tests

Behavioral tests were conducted before and after transplantation monthly until the animals were sacrificed.

Treadscan analysis—We utilized an unbiased treadmill device, TreadScan (Columbus Instruments, Columbus, OH, USA) to detect gait alterations that are reminiscent of locomotion changes seen in Huntington patients. All mice were allowed to walk on the motor-driven treadmill belt at a speed of 15 cm/s for a period of 20s. The foot-prints and body movement were recorded with a high-speed digital video camera from the ventral view of the treadmill belt reflected off the mirror. TreadScan software (CleverSys) was used to identify initial foot contact, stance duration, stride duration, foot liftoff, swing duration, stride length, track width, and toe spread for each foot. The digital data were analyzed to compare each of the parameters between ipsilateral and contralateral sides and between the transplant and non-transplant groups.

Rota-rod test—An accelerating Rotarod (Columbus Instruments, Columbus, OH, USA) was used to test motor coordination. The mouse was placed on a rotating rod that accelerated from 4 rotations per minute (rpm) to 40 rpm in a period of 300 s. The period of time the mouse stayed on the rod was monitored and the 3 of a total of 5 runs in which the mouse performed the best were recorded.

Open field test—Mice were placed in the center of activity chambers equipped with infrared beams (Med ASSOCIATES, St. Albans, VT; 27 \times 27 \times 20.3 cm). Activities were recorded for 30 min under normal conditions of lighting. Quantitative analysis was done on total distance, center ratio and crossings.

Stereological analysis of grafts

Animals were perfused with 4% paraformaldehyde, brains dissected out, and coronal cryosections made at 30 μ m in thickness for free-floating immunostaining (Yang et al., 2008). The number of grafted human cells (hN+) and GABA neurons (GABA+ /DARPP32+/hN+) were counted using a StereoInvestigator software (MicroBrightField, Inc) on every 6 sections as described (Yang et al., 2008). The area of the graft was outlined according to the presence of hN positive cells under a 10 \times objective of a Zeiss fluorescent scope. Cell counting was performed with a 40 \times objective in fields chosen by the software. The number of cells on each section and within the whole graft were estimated by the Stereo Investigator software (Peterson, 1999). Data are presented as mean \pm s.e.m.. (n=10). For measuring GABA neuronal body and processes, we employed NeuronJ (from ImageJ) software to trace fluorescent images of neurons that expressed GABA. Tracings were color coded: red for primary neurite (emanating directly from the soma), blue for secondary neurite (branching from a primary), yellow for tertiary neurite (branching from a secondary), and purple for quaternary neurite (branching from a tertiary).

Statistical analyses

SPSS software was used for statistical analysis. In all studies, comparison of mean values was conducted with unpaired *t* test, one-way ANOVA or repeat measures of general linear model (GLM) analysis. In all analyses, statistical significance was determined at the 5% level ($P < 0.05$).

Supplementary Material

Refer to Web version on PubMed Central for supplementary material.

Acknowledgments

This study was supported in part by the NIH-NINDS (NS045926), the NICHD (P30 HD03352), Ministry of Science and Technology, China (2006CB94700, 2006AA02A101), and Shanghai Municipality (06dj14001).

REFERENCES

- Arlotta P, Molyneaux BJ, Jabaudon D, Yoshida Y, Macklis JD. Ctip2 controls the differentiation of medium spiny neurons and the establishment of the cellular architecture of the striatum. *J Neurosci*. 2008; 28:622–632. [PubMed: 18199763]
- Aubry L, Bugi A, Lefort N, Rousseau F, Peschanski M, Perrier AL. Striatal progenitors derived from human ES cells mature into DARPP32 neurons in vitro and in quinolinic acid-lesioned rats. *Proc Natl Acad Sci U S A*. 2008; 105:16707–16712. [PubMed: 18922775]
- Bachoud-Levi A, Bourdet C, Brugieres P, Nguyen JP, Grandmougin T, Haddad B, Jeny R, Bartolomeo P, Boisse MF, Barba GD, et al. Safety and tolerability assessment of intrastriatal neural allografts in five patients with Huntington's disease. *Exp Neurol*. 2000; 161:194–202.
- Bachoud-Levi AC, Gaura V, Brugieres P, Lefaucheur JP, Boisse MF, Maison P, Baudic S, Ribeiro MJ, Bourdet C, Remy P, et al. Effect of fetal neural transplants in patients with Huntington's disease 6 years after surgery: a long-term follow-up study. *Lancet Neurol*. 2006; 5:303–309.
- Bonner JF, Blesch A, Neuhuber B, Fischer I. Promoting directional axon growth from neural progenitors grafted into the injured spinal cord. *J Neurosci Res*. 2010; 88:1182–1192.
- Campbell K. Dorsal-ventral patterning in the mammalian telencephalon. *Curr Opin Neurobiol*. 2003; 13:50–56.
- Campbell K, Kalen P, Victorin K, Lundberg C, Mandel RJ, Bjorklund A. Characterization of GABA release from intrastriatal striatal transplants: dependence on host-derived afferents. *Neuroscience*. 1993; 53:403–415.
- Clelland CD, Barker RA, Watts C. Cell therapy in Huntington disease. *Neurosurg Focus*. 2008; 24:E9.
- Danjo T, Eiraku M, Muguruma K, Watanabe K, Kawada M, Yanagawa Y, Rubenstein JL, Sasai Y. Subregional specification of embryonic stem cell-derived ventral telencephalic tissues by timed and combinatory treatment with extrinsic signals. *J Neurosci*. 2011; 31:1919–1933.
- Dobrossy MD, Dunnett SB. The effects of lateralized training on spontaneous forelimb preference, lesion deficits, and graft-mediated functional recovery after unilateral striatal lesions in rats. *Exp Neurol*. 2006; 199:373–383.
- Dunnett SB, Rosser AE. Cell transplantation for Huntington's disease Should we continue? *Brain Res Bull*. 2007; 72:132–147.
- Durieux PF, Schiffmann SN, de Kerchove d'Exaerde A. Targeting neuronal populations of the striatum. *Front Neuroanat*. 2011; 5:40.
- Flames N, Pla R, Gelman DM, Rubenstein JL, Puelles L, Marin O. Delineation of multiple subpallial progenitor domains by the combinatorial expression of transcriptional codes. *J Neurosci*. 2007; 27:9682–9695.
- Fode C, Ma Q, Casarosa S, Ang SL, Anderson DJ, Guillemot F. A role for neural determination genes in specifying the dorsoventral identity of telencephalic neurons. *Genes Dev*. 2000; 14:67–80.
- Gallina P, Paganini M, Lombardini L, Mascalchi M, Porfirio B, Gadda D, Marini M, Pinzani P, Salvianti F, Crescioli C, et al. Human striatal neuroblasts develop and build a striatal-like structure into the brain of Huntington's disease patients after transplantation. *Exp Neurol*. 2010; 222:30–41.
- Gerfen CR. Synaptic organization of the striatum. *J Electron Microscop Tech*. 1988; 10:265–281.
- Goto S, Yamada K, Yoshikawa M, Okamura A, Ushio Y. GABA receptor agonist promotes reformation of the striatonigral pathway by transplant derived from fetal striatal primordia in the lesioned striatum. *Exp Neurol*. 1997; 147:503–509.

- Hansson O, Petersen A, Leist M, Nicotera P, Castilho RF, Brundin P. Transgenic mice expressing a Huntington's disease mutation are resistant to quinolinic acid-induced striatal excitotoxicity. *Proc Natl Acad Sci U S A*. 1999; 96:8727–8732.
- Hauser RA, Furtado S, Cimino CR, Delgado H, Eichler S, Schwartz S, Scott D, Nauert GM, Soety E, Sossi V, et al. Bilateral human fetal striatal transplantation in Huntington's disease. *Neurology*. 2002; 58:687–695.
- Hu BY, Du ZW, Li XJ, Ayala M, Zhang SC. Human oligodendrocytes from embryonic stem cells: conserved SHH signaling networks and divergent FGF effects. *Development*. 2009; 136:1443–1452.
- Hu BY, Weick JP, Yu J, Ma LX, Zhang XQ, Thomson JA, Zhang SC. Neural differentiation of human induced pluripotent stem cells follows developmental principles but with variable potency. *Proc Natl Acad Sci U S A*. 2010; 107:4335–4340. [PubMed: 20160098]
- Johnson CD, Davidson BL. Huntington's disease: progress toward effective disease-modifying treatments and a cure. *Hum Mol Genet*. 2010; 19:R98–R102. [PubMed: 20421366]
- Johnson MA, Weick JP, Pearce RA, Zhang SC. Functional neural development from human embryonic stem cells: accelerated synaptic activity via astrocyte coculture. *J Neurosci*. 2007; 27:3069–3077. [PubMed: 17376968]
- Kawaguchi Y, Wilson CJ, Augood SJ, Emson PC. Striatal interneurons: chemical, physiological and morphological characterization. *Trends Neurosci*. 1995; 18:527–535. [PubMed: 8638293]
- Koller WC, Trimble J. The gait abnormality of Huntington's disease. *Neurology*. 1985; 35:1450–1454. [PubMed: 3162109]
- Li XJ, Hu BY, Jones SA, Zhang YS, Lavaute T, Du ZW, Zhang SC. Directed differentiation of ventral spinal progenitors and motor neurons from human embryonic stem cells by small molecules. *Stem Cells*. 2008; 26:886–893. [PubMed: 18238853]
- Li XJ, Zhang X, Johnson MA, Wang ZB, Lavaute T, Zhang SC. Coordination of sonic hedgehog and Wnt signaling determines ventral and dorsal telencephalic neuron types from human embryonic stem cells. *Development*. 2009; 136:4055–4063. [PubMed: 19906872]
- Mazzocchi-Jones D, Dobrossy M, Dunnett SB. Environmental enrichment facilitates long-term potentiation in embryonic striatal grafts. *Neurorehabil Neural Repair*. 2011; 25:548–557. [PubMed: 21444652]
- Menalled L, El-Khodori BF, Patry M, Suarez-Farinas M, Orenstein SJ, Zahasky B, Leahy C, Wheeler V, Yang XW, MacDonald M, et al. Systematic behavioral evaluation of Huntington's disease transgenic and knock-in mouse models. *Neurobiol Dis*. 2009; 35:319–336. [PubMed: 19464370]
- Nakao N, Itakura T. Fetal tissue transplants in animal models of Huntington's disease: the effects on damaged neuronal circuitry and behavioral deficits. *Prog Neurobiol*. 2000; 61:313–338. [PubMed: 10727778]
- Olsson M, Campbell K, Wictorin K, Bjorklund A. Projection neurons in fetal striatal transplants are predominantly derived from the lateral ganglionic eminence. *Neuroscience*. 1995; 69:1169–1182. [PubMed: 8848105]
- Quimet CC, Miller PE, Hemmings HC Jr, Walaas SI, Greengard P. DARPP-32, a dopamine- and adenosine 3':5'-monophosphate-regulated phosphoprotein enriched in dopamine-innervated brain regions. III. Immunocytochemical localization. *J Neurosci*. 1984; 4:111–124. [PubMed: 6319625]
- Palfi S, Conde F, Riche D, Brouillet E, Dautry C, Mittoux V, Chibois A, Peschanski M, Hantraye P. Fetal striatal allografts reverse cognitive deficits in a primate model of Huntington disease. *Nat Med*. 1998; 4:963–966. [PubMed: 9701252]
- Pankratz MT, Li XJ, Lavaute TM, Lyons EA, Chen X, Zhang SC. Directed neural differentiation of human embryonic stem cells via an obligated primitive anterior stage. *Stem Cells*. 2007; 25:1511–1520. [PubMed: 17332508]
- Pearlman S, Levivier M, Gash DM. Striatal implants of fetal striatum or gelfoam protect against quinolinic acid lesions of the striatum. *Brain Res*. 1993; 613:203–211. [PubMed: 8186968]
- Peterson DA. Quantitative histology using confocal microscopy: implementation of unbiased stereology procedures. *Methods*. 1999; 18:493–507. [PubMed: 10491280]

- Pfeifer K, Vroemen M, Blesch A, Weidner N. Adult neural progenitor cells provide a permissive guiding substrate for corticospinal axon growth following spinal cord injury. *Eur J Neurosci.* 2004; 20:1695–1704. [PubMed: 15379990]
- Philpott LM, Kopyov OV, Lee AJ, Jacques S, Duma CM, Caine S, Yang M, Eagle KS. Neuropsychological functioning following fetal striatal transplantation in Huntington's chorea: three case presentations. *Cell Transplant.* 1997; 6:203–212. [PubMed: 9171153]
- Puelles L, Kuwana E, Puelles E, Bulfone A, Shimamura K, Keleher J, Smiga S, Rubenstein JL. Pallial and subpallial derivatives in the embryonic chick and mouse telencephalon, traced by the expression of the genes *Dlx-2*, *Emx-1*, *Nkx-2.1*, *Pax-6*, and *Tbr-1*. *J Comp Neurol.* 2000; 424:409–438. [PubMed: 10906711]
- Reuter I, Tai YF, Pavese N, Chaudhuri KR, Mason S, Polkey CE, Clough C, Brooks DJ, Barker RA, Piccini P. Long-term clinical and positron emission tomography outcome of fetal striatal transplantation in Huntington's disease. *J Neurol Neurosurg Psychiatry.* 2008; 79:948–951. [PubMed: 18356253]
- Rosser AE, Barker RA, Harrower T, Watts C, Farrington M, Ho AK, Burnstein RM, Menon DK, Gillard JH, Pickard J, et al. Unilateral transplantation of human primary fetal tissue in four patients with Huntington's disease: NEST-UK safety report ISRCTN no 36485475. *J Neurol Neurosurg Psychiatry.* 2002; 73:678–685. [PubMed: 12438470]
- Roy NS, Cleren C, Singh SK, Yang L, Beal MF, Goldman SA. Functional engraftment of human ES cell-derived dopaminergic neurons enriched by coculture with telomerase-immortalized midbrain astrocytes. *Nat Med.* 2006; 12:1259–1268. [PubMed: 17057709]
- Sanberg PR, Giordano M, Henault MA, Nash DR, Ragozzino ME, Hagenmeyer-Houser SH. Intraparenchymal striatal transplants required for maintenance of behavioral recovery in an animal model of Huntington's disease. *J Neural Transplant.* 1989; 1:23–31. [PubMed: 2535266]
- Sussel L, Marin O, Kimura S, Rubenstein JL. Loss of *Nkx2.1* homeobox gene function results in a ventral to dorsal molecular respecification within the basal telencephalon: evidence for a transformation of the pallidum into the striatum. *Development.* 1999; 126:3359–3370. [PubMed: 10393115]
- Takahashi K, Tanabe K, Ohnuki M, Narita M, Ichisaka T, Tomoda K, Yamanaka S. Induction of pluripotent stem cells from adult human fibroblasts by defined factors. *Cell.* 2007; 131:861–872. [PubMed: 18035408]
- Thomson JA, Itskovitz-Eldor J, Shapiro SS, Waknitz MA, Swiergiel JJ, Marshall VS, Jones JM. Embryonic stem cell lines derived from human blastocysts. *Science.* 1998; 282:1145–1147. [PubMed: 9804556]
- Toresson H, Campbell K. A role for *Gsh1* in the developing striatum and olfactory bulb of *Gsh2* mutant mice. *Development.* 2001; 128:4769–4780. [PubMed: 11731457]
- Toresson H, Parmar M, Campbell K. Expression of *Meis* and *Pbx* genes and their protein products in the developing telencephalon: implications for regional differentiation. *Mech Dev.* 2000; 94:183–187. [PubMed: 10842069]
- Vandeputte C, Taymans JM, Casteels C, Coun F, Ni Y, Van Laere K, Baekelandt V. Automated quantitative gait analysis in animal models of movement disorders. *BMC Neurosci.* 2010; 11:92. [PubMed: 20691122]
- Wichterle H, Turnbull DH, Nery S, Fishell G, Alvarez-Buylla A. In utero fate mapping reveals distinct migratory pathways and fates of neurons born in the mammalian basal forebrain. *Development.* 2001; 128:3759–3771. [PubMed: 11585802]
- Victorin K. Anatomy and connectivity of intrastriatal striatal transplants. *Prog Neurobiol.* 1992; 38:611–639. [PubMed: 1589583]
- Victorin K, Brundin P, Gustavii B, Lindvall O, Bjorklund A. Reformation of long axon pathways in adult rat central nervous system by human forebrain neuroblasts. *Nature.* 1990; 347:556–558. [PubMed: 1699131]
- Wilburn B, Rudnicki DD, Zhao J, Weitz TM, Cheng Y, Gu X, Greiner E, Park CS, Wang N, Sopher BL, et al. An antisense CAG repeat transcript at JPH3 locus mediates expanded polyglutamine protein toxicity in Huntington's disease-like 2 mice. *Neuron.* 2011; 70:427–440. [PubMed: 21555070]

- Wilson SW, Rubenstein JL. Induction and dorsoventral patterning of the telencephalon. *Neuron*. 2000; 28:641–651. [PubMed: 11163256]
- Yang D, Zhang ZJ, Oldenburg M, Ayala M, Zhang SC. Human embryonic stem cell-derived dopaminergic neurons reverse functional deficit in parkinsonian rats. *Stem Cells*. 2008; 26:55–63. [PubMed: 17951220]
- Yun K, Potter S, Rubenstein JL. Gsh2 and Pax6 play complementary roles in dorsoventral patterning of the mammalian telencephalon. *Development*. 2001; 128:193–205. [PubMed: 11124115]
- Zhang N, An MC, Montoro D, Ellerby LM. Characterization of Human Huntington's Disease Cell Model from Induced Pluripotent Stem Cells. *PLoS Curr*. 2010; 2:RRN1193. [PubMed: 21037797]
- Zhang SC, Wernig M, Duncan ID, Brustle O, Thomson JA. In vitro differentiation of transplantable neural precursors from human embryonic stem cells. *Nat Biotechnol*. 2001; 19:1129–1133. [PubMed: 11731781]

HIGHLIGHTS

1. Directed differentiation of medium spiny GABA neurons from human stem cells;
2. Human GABA neurons grafted into striatum project specifically to the midbrain;
3. Transplanted human GABA neurons reconnect the neural circuitry;
4. Human GABA neuron transplantation corrects motor deficits in Huntington mice.

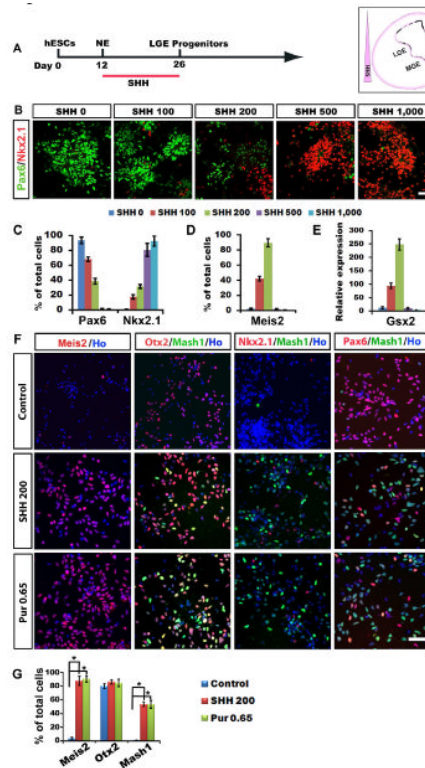


Figure 1. Specification of LGE-like progenitors from hESCs

(A) A schematic procedure for differentiating LGE-like progenitors from hESCs. (B) Pax6-expressing dorsal progenitors decrease while Nkx2.1-expressing ventral progenitors increase in response to increasing concentrations of SHH. (C-E) Quantification of Pax6-, Nkx2.1- (C), Meis2- (D) expressing cell population among total cells and Gsx2 mRNA expression (E) in response to SHH (H9 and H1 cell lines, day 26). (F) Representatives of Meis2-, Mash1-, Nkx2.1-, and Pax6-expressing cells in cultures with medium concentration of SHH (200 ng/ml) or purmorphamine (0.65 μ M). (G) Quantification of Meis2, Otx2, Mash1-expressing cells among total cells in the presence of SHH (200 ng/ml) or purmorphamine (0.65 μ M). Data are presented as mean \pm s.e.m.. (* P <0.05. one-way ANOVA test) Blue, Hoechst-stained nuclei. Scale bars: 50 μ m.

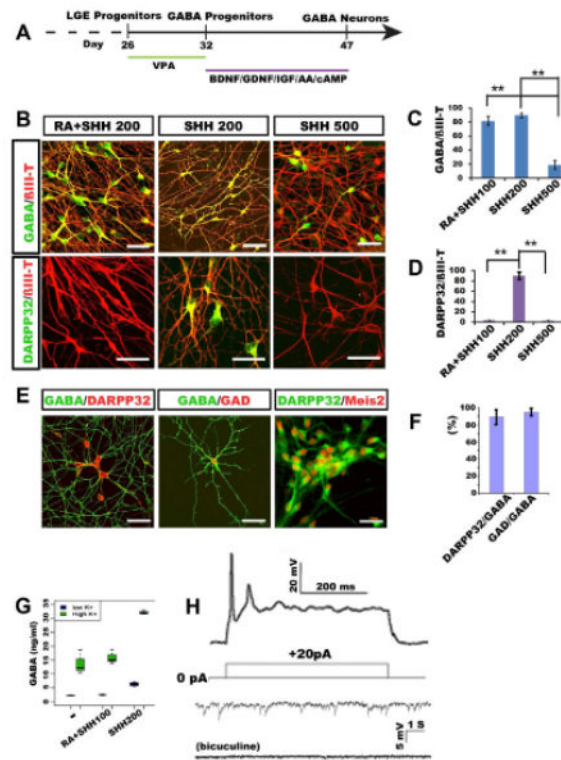


Figure 2. Differentiation and characterization of GABA neurons

(A) Schematic procedure of GABA neuron differentiation. (B) At day 47, GABA-expressing neurons are present in all cultures but DARPP32-expressing GABA neurons are present only in cultures that were treated with 200 ng/ml SHH but not in higher concentrations of SHH or in both RA and SHH. (C, D) Quantification of GABA and DARPP32 cell populations among βIII-tubulin+ neurons under the three culture conditions (200 ng/ml SHH, 500 ng/ml SHH, and RA+200 ng/ml SHH). (E) GABA neurons generated under 200 ng/ml of SHH exhibit spiny morphology and express DARPP32, GAD, Meis2. (F) Quantitative analysis of DARPP32 and GAD positive cells among GABA positive cells. (G) HPLC measurement of GABA release from cultures treated with or without high concentration of potassium. (H) Whole cell patch clamping of neurons differentiated for 10 weeks show action potentials and spontaneous inward synaptic currents which are almost completely eliminated by bicuculine. *P* values (**P*<0.05, ***P*<0.01) in c, d, f and g were determined using the one-way ANOVA test. Data are shown as means±s.e.m.. Scale bars: 50 μm.

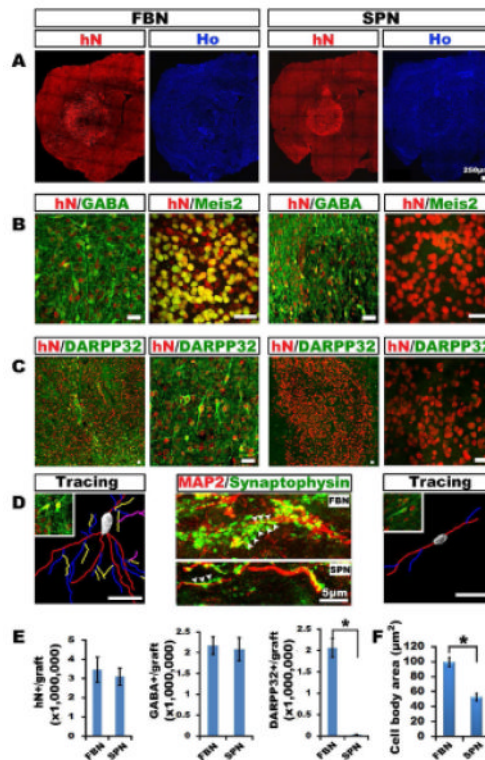


Figure 3. Generation of differential GABAergic neuronal types from grafted human neural progenitors

(A) Grafted human forebrain (FBN) and spinal (SPN) GABA neural progenitors survive for 4 months, as revealed by human nuclei (hN) staining, and do not disrupt striatal structures, as indicated by Hoechst staining. (B) Both FBN and SPN generate GABA neurons but the GABA neurons in the FBN group are positive for Meis2. (C) GABA neurons in the FBN but not SPN grafts express DARPP32. (D) The GABA neurons in the FBN group are larger and more branched, and their dendrites, labeled by MAP2, possess more human-specific synaptophysin+ buttons (arrowheads) than those in the SPN group. (E) Stereological analysis estimates a similar number of total grafted cells and GABA neurons in the FBN and SPN grafts but the majority of GABA neurons in the FBN grafts are positive for DARPP32. Data are means±s.e.m.. (** $P < 0.01$, $n = 10$, one-way ANOVA test) (F) The cell body area of FBN GABA neurons is larger than that of SPN GABA neurons. Data are means±s.e.m.. (** $P < 0.01$, $n = 20$, unpaired t test). Scale bars: 25 µm.

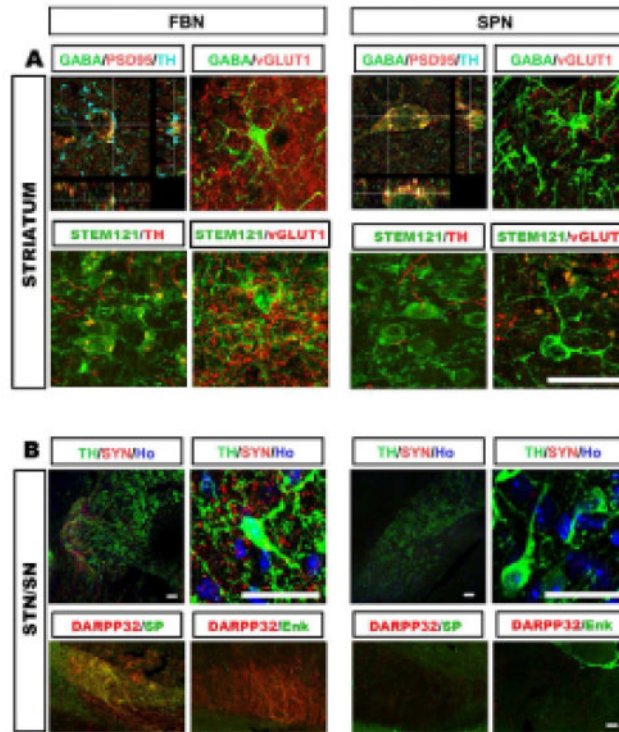


Figure 4. Projection and connections by grafted human GABA neurons

(A) In the striatum, GABA neurons of the FBN but not the SPN grafts possess dense TH⁺ terminals on cell bodies. GABA neurons of both FBN and SPN grafts have vGLUT1 positive terminals but GABA neurons in the FBN grafts have more (upper row). Most of the TH⁺ and vGlu⁺ fibers are negative for human-specific STEM121 (low row). (B) In anterior midbrain (STN/SN), human neuronal fibers, indicated by human specific synaptophysin, are present and surround TH⁺ dopamine neurons in the brain grafted with FBN but not SPN cells. The DARPP32⁺ fibers in the FBN-grafted nigra are also positive for substance P but not enkephalin (lower row). Scale bars: 25 μ m.

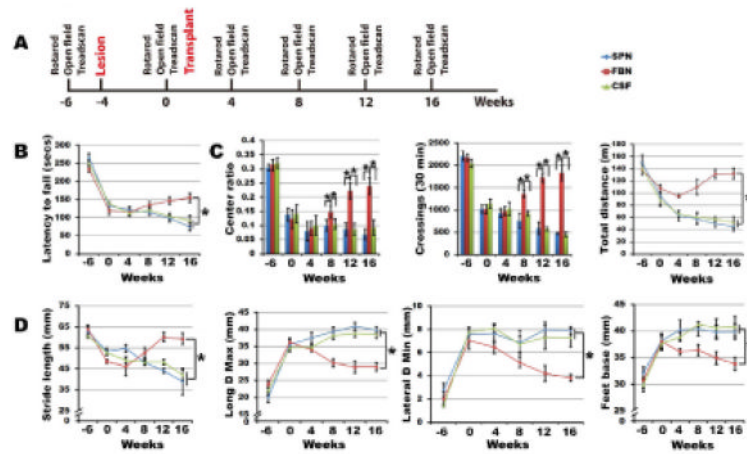


Figure 5. Transplantation of human GABA MSN corrects locomotive deficits

(A) Schematic presentation of temporal course of transplantation and behavioral analysis. (B) Rota-rod tests show increased latency in animals transplanted with FBN but not SPN. (C) Open field tests indicate increased center ratio, crossing times, and distances in animals grafted with FBN but not SPN. (D) Treadscan analysis reveals increased stride length, as well as decreased maximum longitudinal deviation, minimum lateral deviation and the foot base of their rear limbs in animals receiving FBN but SPN grafts. (B) and (D) were analyzed using the repeat measures of general linear model (GLM) analysis, and open field behaviors (E) were analyzed by one-way ANOVA. (* $P < 0.05$, $n = 10$).